International Journal of Advanced Culture Technology Vol.4 No.1 31-36 (2016)
http://dx.doi.org/10.17703/IJACT.2016.4.1.31

IJACT 16-1-5

Numerical Simulation of Phase Separation in Bulk Hetero-junction Photoactive Layer

Nguyen Thi Hang[1], Dinh Van Thuong[1],Hoang Nam Nhat[1] and Dinh Van Chau[1,*]

[1]*Faculty of Engineering Physics and Nanotechnology*
VNU-University of Engineering and Technology
vanchaudinh@gmail.com

Abstract

Morphology evolution of the active layer in bulk hetero-junction organic photovoltaic is modeled and visualized. The width of the phase domain can be predicted using the relationship of characteristics length and evolution time of the process. The 3D numerical simulation of the PCBM/P3HT blend morphology evolution with respect to time is presented. It is observed that the domain width of composition phase can be predicted by using the relationship between value of characteristic length R(t) and evolution time t.

Keywords*: XLPE, Partial discharge, Insulation resistance, Deterioration characteristics, Tanδ*

1. Introduction

Organic photovoltaic (OPV) is considered as a promising alternative to traditional inorganic solar cell due to low cost solar power conversion, printable on flexible substrate, and able to produce at room temperature [1,2]. Many efforts have been done to improve conversion efficiency, a lack point of OPV in comparison with inorganic solar cell, in which architecture is an approach. Bulk heterostructure (BH) showed an enhancement in the efficiency by creating the distributed donor-acceptor junctions accessible within the diffusion length of the light-induced excitons, therefore enabling exciton separation into useful electron-hole pairs before they can disappear through self-recombination [3-5]. Thus it can be said that the morphology of the photonactive layer plays an important role for the efficient operation of the cell. On other hand, the performance of the cell is intimately dictated by its morphology characteristic.

Significant empirical evidences [6-9] showed that the structural randomness in the morphology emerges due to the phase segregation process during the fabrication of the cell. Thus the phase separation process can be modeled by free energy approach with applying Cahn-Hilliard equation [10] for simulation of the morphology evolution with process factors. In practice, the phase-segregation can be achieved by various ways, for example, proper selection of donor/accepter material, composition of those in bend, process conditions like temperature and time annealing or vapor of solvent [11]. The obtained BH morphology using this approach is randomness, interpenetrating clusters of A and D polymer (Figure. 1). During cell operation, photon is absorbed in one or both the A and D phases to create charge neutral particle called exciton. The

Manuscript Received: Feb. 5, 2016 / Revised: Feb. 18, 2016 / Accepted: Mar. 5, 2016
Corresponding Author: vanchaudinh@gmail.com
Tel: +84-04-3754-7461 Fax: +84-04-3754-7460
Faculty of Engineering Physics and Nanotechnology VNU-University of Engineering and Technology

excitons must then diffuse to the interfacial boundary of the A and D phases. At the interface, the excitons can be separated into electrons and holes, then the carriers transported to the respective electrodes to contribute to the output current. During this optoelectronic operation, three cases may occur and affect the performance of dvice: (i) the interface is too far from exciton generation points i.e domain side of cluster, $W_{c,}$ is much larger than diffusion length of exciton ($W_c \sqrt{D_{ex}\tau_{ex}}$), a significant fraction of exciton would be lost by self recombination; (ii) the domain side is too small in comparison with the exciton diffusion length ($W_c \sqrt{D_{ex}\tau_{ex}}$), leading to the larger diffused heterojunction, W_{int}, making quasi electric field at the junction not sufficient to dissociate excitons, resulting in the dissociation rate of exciton would be weak (iii) the photonactive layer thickness (T_{film}) is much larger than the cluster domain side even 100% of excitons is dissociated (W_c ; $\sqrt{D_{ex}\tau_{ex}} T_{film}$), a significant fraction of carrier would be trapped in isolate/wrong connected islands, resulting in loss of the short circuit current and fluctuation of open circuit voltage of the cell. Annealing stage during device fabrication process plays a key to connect the isolated islands to the electrodes. The fraction of total volume connected to appropriate contact for collection of hole, electron, respectively (R_{vol}) the cluster domain side (W_c) and the thickness of hetrojunction interface (W_{int}) may consider as characteristic of the active layer morphology and would be controlled by time- and temperature anneal.

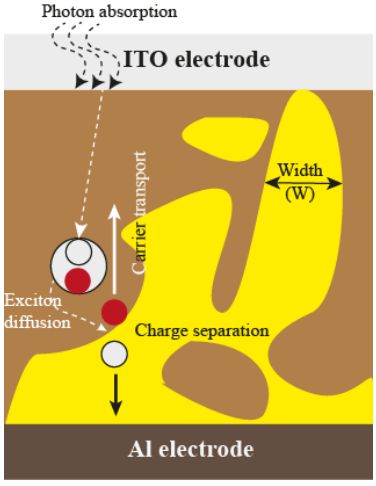

Figure. 1 Schematic of Donor-Acceptor Bulk Hetero-juction Photovoltaic Cell

In this paper, we present a model investigating effects of time and temperature of the annealing stage on morphology characteristic of the BH photoactive layer made of Ethanofullerene Phenyl C61 Butyric Acid Methyl Ester (PCBM) and Poly 3-hexylthiophene-2,5-diyl (P3HT).

2. Mathematics of Model

2.1. Fundamentals

Thermodynamically, behavior of a spinodal decomposition of the PCBM/P3HT blend can be described by Cahn-Hilliard Equation, the free energy, F, with consideration of a surface energy on the substrate is governed by:

$$F(C)\int_V \left\{ f + f_e + \kappa(\nabla C)^2 \right\} dV + \int_S f_s(C, \mathrm{r}) dS \quad (1)$$

where, C is the mole fraction of one polymer component, f is the local free-energy density of homogeneous material, f_e is the elastic energy density, and k is gradient energy coefficient. The term $\kappa(\nabla C)^2$ is the additional free energy density if the material is in a composition gradient.

The free energy variation on the heterogeneously functionalized substrate is simulated by a free energy term, f_s, which is a function if the composition and the coordinates , **r**, as well. The surface free energy is added on the surface of the substrate.

The composition evolution can be written as the function of local composition:

$$\frac{dC}{dt} = \nabla^2 . \left[M \left(\frac{\partial f}{\partial C} + \frac{\partial f_e}{\partial C} - \kappa \nabla^2 C \right) \right] \quad (2)$$

The Flory-Huggins type of free energy is used to model the bulk free energy density as Equation 3:

$$f = \frac{RT}{v_{site}} \left(\frac{C_{PCBM}}{m_{PCBM}} \ln C_{PCBM} + \frac{C_{P3HT}}{m_{P3HT}} \ln C_{P3HT} + \chi_{PCBM/P3HT} C_{PCBM} C_{P3HT} \right) \quad (3)$$

where C_i is the volume fraction of component, m_i is the degree if polymerization of component i, T is the temperature in K, R is the ideal gas constant, χ is the Florin-Huggins interaction parameter between two components depending on temperature, and v_{site} is the molar volume of the reference site in the Flory-Huggins lattice model.

The elasticity is assumed isotropic in the domain. According to the Vergard's law [12], the strees-free strain is isotropic and depends linearly on the composition:

$$e_{ij}^0 = \eta (C - C_0) \delta_{ij} \quad (4)$$

in which e_{ij}^0 is the stress-free strain, C_0 is the average composition of the domain, δ_{ij} is the Kronecker delta function, and h is the compositional expansion coefficient which is expected to be independent of the composition and composition gradient [13]

According to the linear elasticity, the stress δ_{ij} is linear with the change of the strain by Hook's law.

$$\delta_{ij} = c_{ijkl} \left(e_{kl} - e_{kl}^0 \right) \quad (5)$$

where c_{ijkl} represents the isothermal elastic tensor that depending on position and composition. The elastic energy then can be expressed as follows in order of no external anisotropic elastic applied.

$$f_e = \frac{1}{2} c_{ijkl} \left(e_{ij} - e_{ij}^0 \right) \left(e_{kl} - e_{kl}^0 \right) \quad (6)$$

The total strain can be evaluated by the local displacement, **u** [14]

$$e_{ij} = \frac{1}{2} \left(\frac{\partial u_i}{\partial r_j} + \frac{\partial u_j}{\partial r_i} \right) \quad (7)$$

The displacement of the reference lattice is then solved by the equilibrium. Given the fast relaxation time compared to the rate of morphology evolution, it can be assumed that the system is in elastic equilibrium [15].

$$\frac{\partial \sigma_{ij}}{r_j} = 0 \quad (8)$$

2.2. Numerical Methods

Solving the Cahn-Hilliard equation is difficult due to the non-linearity and the bi-harmonic term property of this equation. The cosine transform method is applied to the spatial discretization:

$$\frac{d\hat{C}}{dt} = M\lambda\left(\left\{\frac{\partial f}{\partial C} + \frac{\partial f_e}{\partial C}\right\} - \kappa\lambda\hat{C}\right) \tag{9}$$

where $\hat{C}$ and $\frac{\partial f}{\partial C} + \frac{\partial f_e}{\partial C}$ represents the cosine transform of the respective terms in Equation 4. λ is the approximation of the discrete Laplacian operator in the transform space [16]:

$$\lambda(\mathrm{k}) = \frac{2\sum_i \cos(2\pi k_i) - \sum 2}{(\Delta x)^2} \tag{10}$$

The vector **k** denotes the discretisized spatial element position in all the dimensions. Numerically, $k_i = n_i / N_i$ where n_i is the element in the i^{th} dimension and N_i represents the number of elements in the i^{th} dimension. Δx is the spatial step in the numerical modeling.

By this means, the partial differential equation is transformed into an ordinary differential equation in the discrete cosine space. A semi-implicit method is used to trade off stability, computing time and accuracy. The linear fourth-order operators can be treated impicitly and the none-linear terms can be treated explicitly. The resulting first-order semi implicit scheme is as below:

$$(1 + M\Delta t\kappa\lambda)\hat{C}^{n+1} = C^n - M\Delta t\lambda\left\{\frac{\Delta f(C^n)}{\Delta C} + \frac{\Delta f_e(C^n)}{\Delta C}\right\} \tag{11}$$

A second-order Adams-Bashforth method [17] was also used for the explicit treatment of the non-linear term after the first time step.

$$(3 + 2M\Delta t\kappa\lambda^2)\hat{C}^{n+1} = 4C^n - \hat{C}^{n-1} + 2M\Delta t\lambda\left(\begin{array}{l}\left\{\frac{\Delta f(C^n)}{\Delta C} + \frac{\Delta f_e(C^n)}{\Delta C}\right\} \\ -\left\{\frac{\Delta f(C^{n-1})}{\Delta C} + \frac{\Delta f_e(C^{n-1})}{\Delta C}\right\}\end{array}\right) \tag{12}$$

When the initial condition and the time length are selected, the composition profile of the domain for the second time step can be calculated with Equation 11. After that, the third and following time steps can be calculated with Equation 12. For simplicity and generality, the equations are dimensionalized. The scaling dimensions and time are chosen as follows:

- Characteristic length: $$\bar{L}^2 = \frac{\kappa v_{site}}{RT} \tag{13}$$

- Characteristic time: $$\bar{t} = \frac{\bar{L}_C{}^2 v_{site}}{M_C RT} \tag{14}$$

The parameters are selected according to the corresponding experiment conditions and the literature. The temperature is 393K (120^{o}C), the degree of polymerization of PCBM and P3HT are 100 and 200, the interaction parameter in the Flory-Huggins type of free energy is evaluated as 0.097. The gradient energy coefficient is selected as 6.9E-11 J/m. The diffusivity is about 1E-20m^2/s for general polymers. The mobility of the system can be evaluated.

3. Results and Discussion

3.1. Morphology Evolution

The phase separation takes place only the second derivative of the local free energy respect to composition was negative. It means that the shape of the free energy has to be turned by temperature to quench the mixture into a miscibility gap. A phase separation initiated from a random composition distribution is shown in Figure 2.

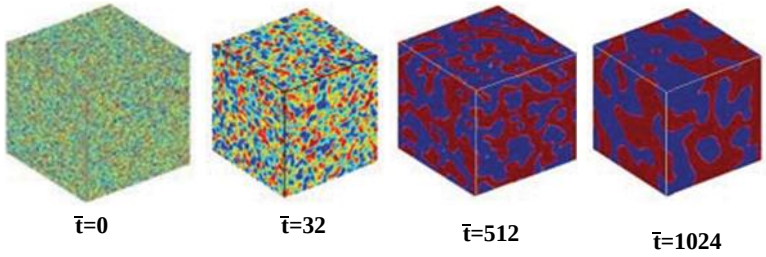

Figure. 2 Morphology Evolution with Respect to Time

It can be seen that the patterns evolve rapidly in the early stage of the phase separation. The gradient in the interface of two phases increases quickly.

3.2. Characteristic Length

Characteristic length of the domain, R(t), must be matched the pattern strips length, lp, of the designed substrate surface in order to optimal polymer self assembly replicating the substrate surface. R(t) measured with respect to time. The domain growth can be governed by evaluating the pair-correlation functions gi in which the subscript represents the directions in the domain:

$$g_i(d,t) = \frac{1}{N_j}\sum_{k_j=1}^{N_j} g_{i,k_j}(d,t) \tag{15}$$

Theoretically, when the spinodal decomposition occurred in the binary polymer mixture, the average characteristic lengths are the same in all directions. The relationship of the characteristic length and time is showed in Figure 3.

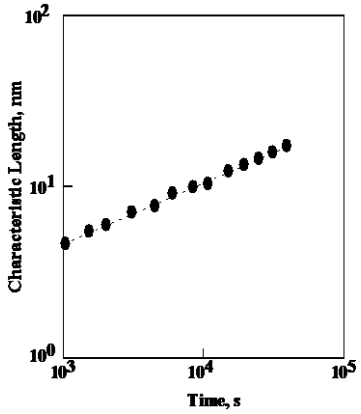

Figure. 3 Domain Width with Respect to Annealing Time

As seen in the Figure 3, the R(t) value can be fitted in a straight line. It shows that about 2.5h of annealing process may be need to obtain the morphology having domain width of 10nm.

4. Conclusions

The 3D numerical simulation of the PCBM/P3HT blend morphology evolution with respect to time is presented. It is observed that the domain width of composition phase can be predicted by using the relationship between value of characteristic length R(t) and evolution time t.

References

[1] M. Helgesen, R. Sondergaard, F.C. Krebs, Advanced materials and processes forpolymer solar cell devices, J. Mater. Chem. 20 (2010) 36–60.
[2] F.C. Krebs, Fabrication and processing of polymer solar cells: a review ofprinting and coating techniques, Sol. Energy Mater. Sol. Cells 93 (2009) 394–412.
[3] Jingbi You, Letian Dou, Ken Yoshimura, Takehito Kato and et al, A polymer tandem solar cell with 10.6% power conversion efficiency, Nature Communications 4, 2013
[4] J. Gilot, et al., "On the efficiency of polymer solar cells," Nature Materials, vol. 6, pp. 704-704, Oct. 2007.
[5] J. D. Servaites, et al., "Practical efficiency limits in organic photovoltaic cells: Functional dependence of fill factor and external quantum efficiency," Applied Physics Letters, Oct. 2009.
[6] R. Giridharagopal and D. S. Ginger,"Characterizing Morphology in Bulk Heterojunction Organic Photovoltaic systems," Journal of Physical Chemistry Letters, pp. 1160-1169, Apr. 2010.
[7] H. Hoppe and N. S. Sariciftci, "Morphology of polymer/fullerene bulk heterojunction solar cells," Journal of Materials Chemistry, vol. 16, pp. 45-61, 2006.
[8] S. Oosterhout, et al., "The effect of threedimensional morphology on the efficiency of hybrid polymer solar cells," Nature Materials, pp. 818-824, Oct. 2009.
[9] J. A. Renz, et al., "Multiparametric optimization of polymer solar cells: A route to reproducible high efficiency," Solar Energy Materials and Solar Cells, pp. 508-513, Apr. 2009.
[10] P. G. de Gennes, "Dynamics of fluctuations and spinodal decomposition in polymer blends," Journal of Chemical Physics, vol. 72, pp. 4756-4763, 1980.
[11] F. C. Krebs, "Fabrication and processing of polymer solar cells: A review of printing and coating techniques," Solar Energy Materials and Solar Cells, vol. 93, pp. 394-412, Apr. 2009.
[12] L. Vegard, The constitution of mixed crystals and the space occupied by atoms. Phys, 1921. 5(17).
[13] A.R. Denton and N.W. Ashcropt, Vergard's law. Physical Review A, 1991. 43(6):p. 3161-3164.
[14] AG. K., Theory of structural transformations in solid. 1983, New York: Wiley.
[15] D.J. Seol et al., Computer simulation of spinodal decomposition in constrained films. Acta Maerialia, 2003, 51(17): p. 5173-5185.
[16] M.L.M. Copetti and C.M. Elliot, kinetics of phase decomposition process: Numerical solutions to Cahn-Hilliard Equation, Material Science and Technology. 1990. 6: p. 279-296.
[17] R. Mauri, R. Shinnar and G. Triamtafyllow, Spinodal decomposition in binary mixtures. Physical Review E, 1996. 53(3): p. 2613-2623.